Heteroatom Chemistry
Volume 11, Number 1, 2000

NMR Study of Spirophosphoranes Derived from 2-Aminophenols

Julio Hernández-Díaz,[1] Rosalinda Contreras,[1]
and Bernd Wrackmeyer[2]

[1]*Departamento de Química, Centro de Investigación y de Estudios Avanzados del IPN, A.P. 14-740, México D.F., 07000 México*

[2]*Laboratorium für Anorganische Chemie, Universität Bayreuth, D-95440 Bayreuth, Germany*

Received 24 June 1999; revised 23 September 1999

ABSTRACT: *Multinuclear magnetic resonance experiments were performed (^{1}H, ^{13}C, ^{31}P, and ^{15}N) for P-H phosphoranes derived from 2-aminophenol, 4-tert-butyl-2-aminophenol, and 4,6-di-tert-butyl-2-aminophenol. Selective heteronuclear $^{1}H\{^{15}N\}$ double resonance experiments and two-dimensional $^{15}N/^{1}H$ HETCOR experiments enabled us to determine various signs of coupling constants (e.g., $^{2}J(^{31}P, N, ^{1}H) > 0$; $^{1}J(^{31}P, ^{15}N) < 0$). The ^{1}H-coupled ^{15}N NMR spectrum recorded by the INEPT pulse sequence shows the splitting due to $^{1}J(^{31}P, ^{15}N)$ and $^{2}J(^{15}N, P, ^{1}H)$. The latter value is useful for polarization transfer experiments from ^{1}H to ^{15}N, once the hydrogen atoms of the N-H functions are replaced by other groups. Isotope-induced chemical shifts $^{1}\Delta^{14/15}N(^{31}P)$ were measured by using the INEPT-HEED pulse sequence.* © 2000 John Wiley & Sons, Inc. Heteroatom Chem 11:11–15, 2000

INTRODUCTION

Spirophosphoranes are pentacoordinated helicoidal compounds that can adopt geometries between a square pyramid and a trigonal bipyramid. The spirophosphoranes bearing nitrogen atoms linked to the phosphorus atom are adequate models for the study of the nature of the P-N bond, which can be different depending on the apical or equatorial positions [1]. Due to the strong Lewis acidity of the phosphorus(V) atom [2–4], the more efficient electron-donor atoms occupy equatorial sites; in this position the surroundings of the nitrogen atom become trigonal planar due to a retrocoordinative π bond from the nitrogen to the phosphorus atom [5]. The π bonding that occurs only for equatorial donor atoms is due to the electrodeficient character of the phosphorus(V). The Lewis-acid behavior of the pentacoordinated phosphorus atom is also shown by its coordination to Lewis bases to give hexacoordinated phosphorus derivatives [3–4]. Indirect nuclear spin-spin coupling constants associated with the system $P(V)H(NRH)_2$ could give information about the bonding situation. Therefore, we were interested in the ^{15}N and ^{31}P NMR parameters of the spirophosphoranes **1–3**.

The compounds **1–3** were prepared according to the literature [6] from the reaction of the corresponding 2-aminophenol with tris(dimethylamino)-phosphane [$P(NMe_2)_3$] in toluene, followed by recrystallization from toluene; the yields were quantitative. The phosphoranes **1–3** exist in a racemic mixture of the two helicoidal structures with oxygen in apical and nitrogen atoms in equatorial positions, as is shown by the X-ray structural analysis

---

Correspondence to: Rosalinda Contreras and Bernd Wrackmeyer.

Contract Grant Sponsor: DAAD.
Contract Grant Sponsor: Cinvestov-IPN.

Dedicated to Prof. Alfred Schmidpeter on the occasion of his 70th birthday.

of compound **1**, [7]. The synthesis of compound **1** is known [6], and its ^{13}C NMR data have recently been reported [1]. Compounds **2–3** are new. The ^{1}H, ^{13}C, ^{15}N, and ^{31}P NMR parameters of the bicyclic phosphoranes **1–3** are given in the Tables 1–3.

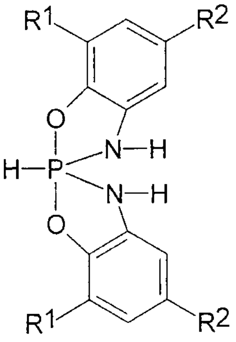

	1	**2**	**3**
R1	H	H	tBu
R2	H	tBu	tBu

DISCUSSION

The composition, stereochemistry, and dynamics of aminophosphoranes are readily revealed by routine ^{1}H, ^{13}C^{1}, and ^{31}P [8] NMR measurements. However, ^{15}N NMR parameters have been measured only for a few examples, mainly aminofluorophosphoranes [9,10], and systematic trends are not obvious at present. One aminofluorophosphorane **4** derived from a 2-aminophenol has been studied by ^{15}N NMR ($^{1}J(^{31}\mathrm{P}, ^{15}\mathrm{N}) = 35.3$ Hz; $\delta^{15}\mathrm{N} = -313.0$) [10].

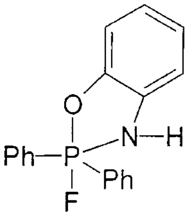

4

Many ^{15}N NMR parameters can be obtained taking advantage of the ^{15}N satellites in the ^{1}H NMR spectra of **1–3**, which represent the A part of an ABMX spin system (A, B = ^{1}H, M = ^{31}P, and X = ^{15}N, with A linked to ^{15}N and B to ^{14}N). A positive sign of the reduced-coupling constants $^{1}K(^{31}\mathrm{P}, ^{15}\mathrm{N})$ [that means $^{1}J(^{31}\mathrm{P}, ^{15}\mathrm{N}) < 0$ because of $\gamma(^{15}\mathrm{N}) < 0$) with respect to $^{1}K(^{15}\mathrm{N}, ^{1}\mathrm{H}) > 0$ [11] was determined by selective heteronuclear ^{1}H{^{31}P} double resonance experiments observing differential effects on the ^{15}N satellite signals (Figure 1). This is in agreement with previous findings for aminofluorophosphoranes [9], in which the amino group is also in an equatorial position, although the absolute magnitude of $|^{1}J(^{31}\mathrm{P}, ^{15}\mathrm{N})|$ is much larger in the latter compounds. This trend, now becoming obvious by the new data for **1–3**, is in line with expectations: positive contributions to

TABLE 1 ^{13}C NMR Data for **1–3**, in C_6D_6 and $CDCl_3$, [J(PC)]

	1	**2**	**3**
C1 C_6D_6	148.2	145.9	143.2
C1 $CDCl_3$		145.4	143.2
C2 C_6D_6	131.0 [16.5]	130.4 [16]	130.7 [16.1]
C2 $CDCl_3$		130.2 [16]	130.4 [16.1]
C3 C_6D_6	110.1 [15.4]	107.7 [15]	105.9 (15.4)
C3 $CDCl_3$		107.5 [14.5]	105.5 [14.6]
C4 C_6D_6	121.0	142.6	142.0
C4 $CDCl_3$		143.8	142.3
C5 C_6D_6	120.0	116.9	114.2
C5 $CDCl_3$		117.0	114.7
C6 C_6D_6	109.9 [5.6]	108.8 [6.2]	131.1 [4.6]
C6 $CDCl_3$		109.0 [6.2]	131.6 [4.6]
C7 C_6D_6		34.3	34.5
C7 $CDCl_3$		34.5	34.7
C8 C_6D_6		31.6	31.7
C8 $CDCl_3$		31.7	31.9
C9 C_6D_6			34.2
C9 $CDCl_3$			34.5
C10 C_6D_6			29.7
C10 $CDCl_3$			29.8

TABLE 2 ^{1}H NMR Data for **1–3**

	1	**2**	**3**
H3 C_6D_6	6.25	6.35	6.27
^{3}J(HH)	7.2		
^{4}J(HH)			1.12, 0.71
H3 $CDCl_3$		6.76	6.85
H4 C_6D_6	6.76		
^{3}J(HH)	7.4, 7.76		
H5 C_6D_6	6.70	6.79	7.03
^{3}J(HH)	7.59, 7.4	8.15	
^{4}J(HH)		1.97	2.19
H5 $CDCl_3$		6.81	6.97
^{3}J(HH)		7.91	
^{4}J(HH)		2.09	
H6 C_6D_6	6.82	6.83	
^{3}J(HH)	7.23	8.15	
H6 $CDCl_3$		6.71	
^{3}J(HH)		7.91	
H8 C_6D_6		1.29	1.37
H8 $CDCl_3$		1.28	1.46
H10 C_6D_6			1.56
H10 $CDCl_3$			1.60
N-H C_6D_6	4.30	4.37	4.53
^{2}J(PH) C_6D_6	19.0	18.8	18.3
N-H $CDCl_3$		4.97	4.97
^{2}J(PH) $CDCl_3$		18.6	17.6
P-H C_6D_6	8.48	8.79	8.81
^{1}J(PH) C_6D_6	829	829.3	815.4
P-H $CDCl_3$		8.89	9.09
^{1}J(PH) $CDCl_3$		834.0	823.9

${}^{1}K({}^{31}P, {}^{15}N)$ (in the absence of a lone pair of electrons at the phosphorus atom) should increase with increasing electronegativity of the other substituents at phosphorus as the result of increasing s-electron density in the P-N hybrid bond orbital, as predicted by Bent's model of rehybridization [12]; the effect is greatest for fluorine atoms in equatorial positions. A positive sign of ${}^{2}J({}^{31}P, N, {}^{1}H)$ (relative to ${}^{1}J({}^{31}P, {}^{15}N) < 0$) follows either from selective heteronuclear ${}^{1}H\{{}^{15}N\}$ double-resonance experiments by observation of differential effects on the ${}^{15}N$ satellite signals or by a 2D ${}^{15}N/{}^{1}H$ HETCOR experiment (Figure 2). The ${}^{1}H$-coupled ${}^{15}N$ NMR spectrum (Figure 3), recorded by the INEPT pulse sequence [13] (based on ${}^{1}J({}^{15}N, {}^{1}H) = 94$ Hz), shows the splitting due to ${}^{1}J({}^{31}P,$

TABLE 3 ${}^{31}P$ and ${}^{15}N$ NMR Data for **1–3**

	1	**2**	**3**
$\delta\ {}^{31}P$ C_6D_6	−47.8	−46.7	−47.9
$\delta\ {}^{31}P$ $CDCl_3$		−46.5	−48.0
${}^{1}J(PH)$ C_6D_6	829.0	828.3	815.4
${}^{1}J(PH)$ $CDCl_3$		835.0	823.7
${}^{2}J(PH)$	17.2	20.1	17.8
${}^{2}J(PH)$		18.4	17.4
$\delta\ {}^{15}N$ C_6D_6	−301.4	−300.7	−301.4
$\delta\ {}^{15}N$ $CDCl_3$		−301.6	
${}^{1}J(PN)$ C_6D_6	27.6	26.7	28
${}^{1}J(PN)$ $CDCl_3$		27.4	
${}^{1}J(NH)$ C_6D_6	+93.6	+93.0	+92.6
${}^{1}J(NH)$ $CDCl_3$		+93.8	

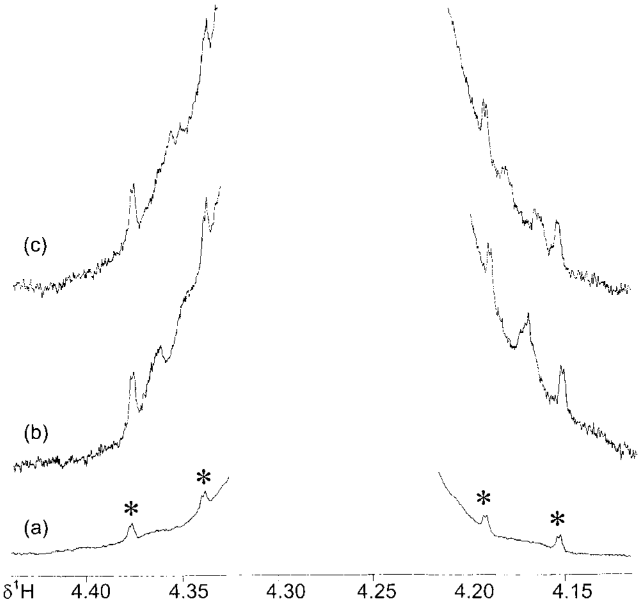

FIGURE 1 Selective heteronuclear ${}^{1}H\{{}^{31}P\}$ double-resonance experiments (active spins ${}^{1}H$, ${}^{31}P$; passive spin, ${}^{15}N$), carried out for **1** in C_6D_6, observing the ${}^{15}N$ satellite signals of the NH resonance: (a) normal spectrum; (b) selective irradiation of the low-frequency transition of one of the triplets in the ${}^{31}P$ NMR spectrum; (c) selective irradiation of the high-frequency transition of one of the triplets in the ${}^{31}P$ NMR spectrum. The differential response to the ${}^{31}P$ irradiation experiments proves that the signs of ${}^{1}K({}^{15}N, {}^{1}H)$ (>0) and ${}^{1}K({}^{31}P, {}^{15}N)$ are alike.

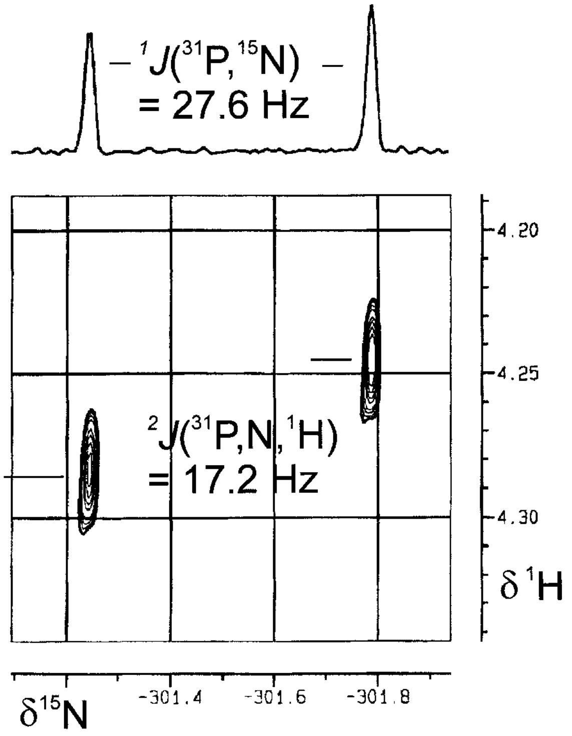

FIGURE 2 Contour plot of the 50.8 MHz 2D ${}^{15}N/{}^{1}H$ HETCOR experiment (64 experiments, 64 transients each; acquisition time 1.5 sec, repetition delay 2 sec zero filling in both dimensions) for **1** in C_6D_6. The positive tilt of the doublet cross peaks shows that the signs of ${}^{1}K({}^{31}P, {}^{15}N)$ and ${}^{2}K({}^{31}P, N, {}^{1}H)$ are alike (both > 0).

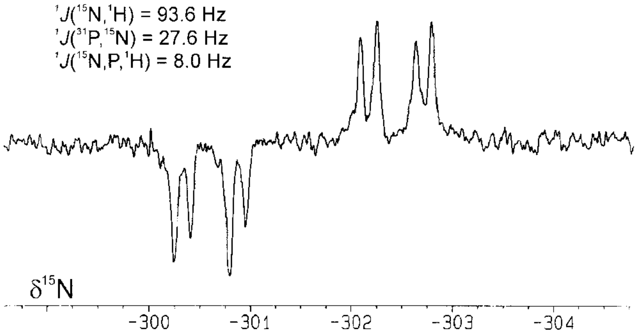

FIGURE 3 ${}^{15}N$ NMR spectrum (50.8 MHz) of **1** in C_6D_6 recorded by using the basic INEPT pulse sequence [10] based on ${}^{1}J({}^{15}N, {}^{1}H)$, without ${}^{1}H$ decoupling.

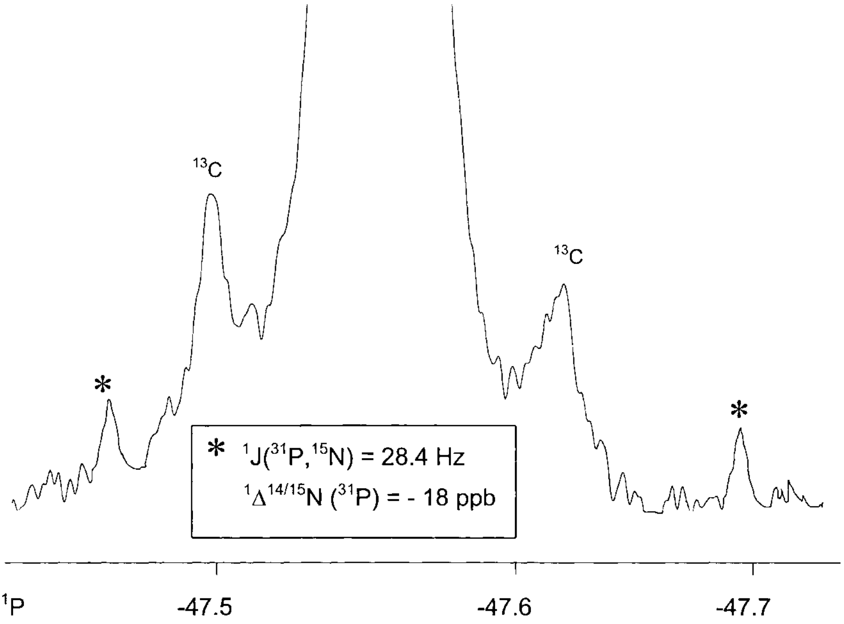

FIGURE 4 ^{31}P{^{1}H} NMR spectrum of **3** in C_6D_6, recorded by using the refocused INEPT-HEED pulse sequence [14] (Hahn-echo delay 0.2 sec). ^{13}C satellites overlap, and the ^{15}N satellites (marked by asterisks) are readily identified both by the isotope-induced chemical shift $^{1}\Delta^{14/15}$N(^{31}P) = −18.0 ppb and the magnitude of $^{1}J(^{31}$P, ^{15}N), in agreement with the data from the ^{15}N NMR spectrum 1–3.

^{15}N) and $^{2}J(^{15}$N, P, ^{1}H). The latter value will be useful for polarization transfer experiments from ^{1}H to ^{15}N, once the hydrogen atoms of the N-H functions are replaced by other groups.

Finally, the isotope-induced chemical shifts $^{1}\Delta^{14/15}$N(^{31}P) were obtained for **2** and **3** by using the INEPT-HEED pulse sequence [14]. Although the ^{15}N satellite signals (^{15}N-^{31}P-^{14}N isotopomer) are still broadened (Figure 4) due to scalar ^{31}P-^{14}N interactions, they are somewhat sharper than the parent signal arising from the ^{14}N-^{31}P-^{14}N isotopomer, which reflects interactions of the ^{31}P nucleus with two spin-1 nuclei [15]. This is the first time that such data have been obtained for aminophosphoranes in natural abundance of ^{15}N. The values $^{1}\Delta^{14/15}$N(^{31}P), as expected, are significantly less negative than for P(III)-nitrogen compounds and in the same order of magnitude as for other phosphorus(V) compounds [16], taking into account general trends described for isotope induced chemical shifts [17].

The ^{15}N resonances of the compounds **1–3** (δ^{15}N-300.7–301.6) are shifted to higher frequencies compared with that of aniline (−323.8 ppm, [18a]). This deshielding effect indicates delocalization of the nitrogen lone pair of electrons not only into the benzene ring but also toward the phosphorus atom. The values $^{1}J(^{15}$N, ^{1}H) are characteristic of the nature of the bonding of nitrogen to other elements. In the case of **1–3** ($^{1}J(^{15}$N, ^{1}H) = −92.6 to −93.8 Hz) the coupling constants are larger in absolute values than for anilines [18b,c] (aniline: −78 Hz and [PhNHPMe$_3$]$^+$ −83.3 Hz). This is in agreement with sp^2 hybridization of the nitrogen atom. Furthermore, the increase in the absolute magnitude of these coupling constants indicates that the nitrogen atom in the phosphoranes is linked to a strongly electronegative center (the phosphorus atom, in this case, is electron-deficient and fairly electronegative at the same time, similar magnitudes of ^{1}J(^{15}N, ^{1}H) are observed, e.g., in phenylhydrazines). The reduced coupling constants $^{1}K(^{31}$P, ^{15}N) become less negative when the lone pair of electrons at the phosphorus atom becomes engaged in bonding, for example, to a transition-metal fragment, a borane, or to a chalcogen. In the case of phosphoranes, it appears that $^{1}K(^{31}$P, ^{15}N) values are positive in general, since negative contributions to the Fermi contact term are smaller than in other phosphorus(V) compounds. The relevance of the article is that now we know the signs of the coupling constants and have an idea about their magnitude. The next step will be to change the substitution pattern of the aminophosphoranes and study the influence on the coupling constants. It will help to discuss the electronic structure of aminophosphoranes. It must be emphasized that such discussion would be meaningless without knowing the signs of the coupling constants.

EXPERIMENTAL

All compounds were characterized by 1D ^{1}H, ^{13}C, ^{15}N, and ^{31}P NMR spectroscopy and by 2D $^{13}C/^{1}H$ and $^{15}N/^{1}H$ HETCOR experiments performed on Jeol GSX 270, Jeol Eclipse 400, Bruker DRX 300, and DRX 500 instruments. The reactions were performed under a nitrogen atmosphere; oven-dried glassware and dry solvents were used. The EI mass spectra (20 eV) were obtained with a HP 5958 spectrometer. Melting points were determined in a Melt-Temp II apparatus and are uncorrected.

Synthesis of Tetra-tert-butyl-2,3,7,8-dibenzo-4,9-diaza-1,6-dioxa-5(H)-phospha(V)spiro[4,4] nonane **3***: General Procedure*

To a solution of 1 g (4.5 mmol) of 4,6-di-*tert*-butyl-2-aminophenol in 20 mL of toluene, 0.36 g (0.40 mL, 2.2 mmol) of $P(NMe_2)_3$ was added. The reaction mixture was refluxed for 4 hours, and three equivalents of evolved dimethylamine were titrated with HCl (1.0 M). After filtration, the solvent was removed in a vacuum. Light yellow crystals were obtained in a quantitative yield (0.96 g; m.p. 188–190 °C). Mass spectra: *m/e* (%) 470.30 (48), 471.3 (16), 469.45 (6), 250.25 (21), 222.30 (26), 221.25 (100), 206.25 (29), 164.2 (6). Calcd. for $C_{28}H_{43}N_2O_2P\cdot 1/2C_7H_8$(516.70): C, 73.22; H, 9.16; N, 5.42. Found: C, 72.89; H, 9.03; N, 4.55.

Compound **2**: quantitative yield of brown crystals, m.p. 189–190 °C. Mass spectra: *m/e* (%) 358.4 (16), 194.3 (13), 166.4 (12), 165.35 (100), 164.40 (9), 150.2 (45). Calcd. for $C_{20}H_{27}N_2O_2P$(358.41): C, 67.02; H, 7.59; N, 7.81. Found: C, 66.39; H, 7.52; N, 7.80.

ACKNOWLEDGMENTS

J.H-D. is grateful to Conacyt-Mexico for a Ph.D. scholarship.

REFERENCES

[1] Tlahuextl, M.; Martínez-Martínez, F. J.; Rosales-Hoz, M. J.; Contreras, R. Phosphorus Sulfur Silicon Relat Elem 1997, 123, 5.
[2] Cong, C. B.; Gence, G.; Garrigues, B.; Koening, M.; Muñoz, A. Tetrahedron 1979, 35, 1825.
[3] Wong, C. Y.; Kennepohl, D. K.; Cavell, R. G. Chem Rev 1996, 96, 1917.
[4] Chuit, C.; Reyé, C. Eur J Inorg Chem 1998, 1847.
[5] Wasada, H.; Hirao, K. J Am Chem Soc 1992, 114, 16.
[6] Ferekh, J.; Brazier, J. F.; Muñoz, A.; Wolf, R. C R Acad Sci 1970, 270c, 865.
[7] Meunier, P. F.; Day, R. O.; Devillers, J. R.; Holmes, R. R. Inorg Chem 1978, 77, 3270.
[8] Cavell, R. G. In Phosphorus-31 NMR Spectroscopy in Stereochemical Analysis; Verkade, J. G., Quin, L. D., Eds.; VCH: Weinheim, 1987; Chapter 7.
[9] (a) Arnold, D. F.; Rankin, D. W. H. J Chem Soc Dalton Trans 1976, 1131; (b) Rankin, D. W. H.; Wight, J. G. J Chem Soc Dalton Trans 1980, 2049; (c) Rankin, D. W. H.; Wight, J. G. J Chem Soc Dalton Trans 1979, 1070.
[10] Stegmann, H. B.; Dumm, H. V.; Scheffer, K. Phosphorus Sulfur Silicon Relat Elem 1978, 5, 159.
[11] Jameson, C. J. In Multinuclear NMR; Mason, J., Ed.; Plenum Press: New York, 1987; Chapter 4.
[12] Bent, H. A. Chem Rev 1961, 61, 275.
[13] Morris, G. A.; Freeman, R. J Am Chem Soc 1979, 101, 760.
[14] Kupce, E.; Wrackmeyer, B. J Magn Reson 1992, 97, 568.
[15] Wrackmeyer, B.; Köhler, C.; Kupce, E. Magn Reson Chem 1993, 31, 769.
[16] Gombler, W.; Kinas, R. W.; Stec, J. W. Z Naturforsch Teil B 1983, 38, 815.
[17] Jameson, C. J. Isotopes in the Physical and Biomedical Sciences; In Buncel, E., Jones, J. R., Eds.; Elsevier: New York, 1991; Vol. 2, pp 1–54 and references cited therein.
[18] (a) Witanowski, M.; Stefaniak, L.; Webb, G. A. Annu Rep NMR Spectrosc 1981, 11b, 198; (b) Witanowski, M.; Stefaniak, L.; Webb, G. A. Annu Rep NMR Spectrosc 1981, 11b, 402; (c) Martin, G. J.; Martin, M. L.; Gouesnard, J.-P. In ^{15}N NMR Spectroscopy, NMR Basis Principles and Progress; Diehl, P., Fluck, E., Kosfed, R., Eds.; Springer Verlag: Berlin, 1981; Vol. 18, pp 254–258.